/Volume 3(1),2025, Page 62-70

Enhancing the Structural Characteristics of Copper Oxide Films by Plasma Technique

Mohammed Shareef Mohammed,

Samarra university- College of education-physics department, Iraq,

mohammed.sh.p@uosamarra.edu.iq

Abstract: In this paper X-ray diffraction examinations showed the appearance of three different phases, Cu, and the crystallization size was 47.99, 48.77, and 30.17 for the CCuITO sample (10, 20, 30), respectively.

As for the density of dislocations, it decreased from the first sample from 4.43 x 1014 lin/m2 to 4.21 x 1014 lin/m2, while the third sample was 1.1 x 1015 lin/m2. As for the mesh stress, it had the same behavior as the density of dislocations, as for the first and second samples it decreased from 0.0028 to 0.0027, while It increased for the third sample to reach 0.0044 The results of the AFM images showed that the average grain size distribution on the surface was 0.119, 0.117, and 0.125 micrometers for the three samples, respectively, while the roughness increased for the first and second samples from 53.55 to 87.771 nanometers, but it increased slightly for the third sample to reach 67.003 nanometers. SEM image results showed that the grain size increased with increasing plasma treatment time, rising from 82.2 to 105 nm with an increase in agglomerations.

Keywords: electron microscope (SEM), X -rays diffraction, Hall effect, chemical composition

1. Introduction

Recently, copper has become the primary focus of integrated circuit metallurgy replacing aluminum due to its higher electrical and thermal conductivity, higher melting temperature, and thus lower diffusion rates. These advantages have attracted important research in the fields of copper film deposition, characterization, and film quality improvement through customized deposition techniques [1]. Copper is electroplated for many engineering and decorative applications that require a wide range of mechanical and physical properties. This range extends from properties superior to fully annealed and wrought copper to properties equivalent to pure annealed copper, and resistivity, modulus of elasticity and coefficient of thermal expansion are important physical properties that can be controlled. These properties are obtained when choosing

Copyright: © 2023 by the authors. Submitted for possible open access publication under the terms and conditions of the Creative Commons Attribution (CC BY) license (https://creativecommons.org/licenses/by/4.0/).

deposition or coating solutions, when choosing the electrochemical deposition method and choosing the operating conditions correctly [2, 3]. Copper is the metal of choice for interconnects because it addresses issues such as integrated circuit performance with the continuing trend toward device miniaturization, and successful applications of copper electrode position in Nano scale interconnects can depend strongly on its dispersive surface roughness. The increase in electronic resistance due to surface dispersion is a fundamental problem in quantum mechanics, while the elimination of surface roughness dispersion and grain boundary dispersion is a morphological problem that can be controlled by fabrication technology [4]. Strengthening these metal films by various methods such as grain size reduction, solid solution strengthening and cold working results in high strength but low electrical conductivity. For example, copper with two or three times higher strength (achieved by alloying), typically has a loss in conductivity of about 50 to 60 percent compared to pure copper. The primary source of strengthening of thin films is the confinement of dislocation movement. Prove entry defects, such as grain boundaries and sediments, it is an effective technique to greatly enhance the mechanical strength. But these defects also act as a very strong scattering site for electrons, and thus lead to low electrical conductivity. This dilemma has led to the exploration of a different type of defect, the double boundary. Twin boundaries act as barriers to dislocation motion in a manner similar to grain boundaries, but the electrical dispersion coefficient at coherent twin boundaries is approximately one order of magnitude lower than that at grain boundaries. There is therefore great potential in designing high-strength, high-conductivity copper films by double-crossing. Copper thin films are also used in multi-layer sandwiches of hard disk read heads [5] GMR. Among the various methods for depositing copper in the form of thin films on substrates such as PVD, CVD, and plasma spraying [6], electrochemical methods have proven to be inexpensive, highly productive, and can be easily adopted [7]. Electrophoretic deposition of materials allows the formation of thin layers, such as monolayers, with the added advantage of better kinetic control [8]; This is expected since there is effective control over the monolayer coverage of the deposited material. Electrode position of copper from cyanide solutions is a well-established industrial practice [9-10]. But this process is now used infrequently, not only because of its toxicity but also because of photoresist attack during the coating process.

Expermintal:

Atmospheric pressure plasma device

The DBD system used in this study was designed and manufactured by our team in Figure (1) It consists of two electrodes, each 50 mm in diameter, and is made of a copper rod surrounded by Teflon for insulation. A one-millimeter thick quartz slab was used as an insulating material between two electrodes. The bottom electrode was connected to a moving stage that allowed the distance between two electrodes to be varied.

The electrodes were connected to a high voltage transformer with an output voltage ranging from (1-15 kV).

Treating copper membrane samples with CAP The surface of the copper nanofilms was modified by exposing it to a dielectric barrier discharge plasma, and each sample was divided into three pieces, and

one of the two copper samples was left without exposure to plasma as a control (t = 0). The other

three samples were exposed to different durations of plasma (10 and 20 minutes). Each sample was placed in an insulating holder manufactured for this purpose. The holder and sample are placed on the bottom electrode of the DBD system. The distance between the surface of the prepared sample and the high electrode of the plasma was 1 mm and the applied voltage was 12 k.

Table (1) Parameters extracted from cyclic stress test chart

ITEM	E red. (V)	Eox. (V)	OCP (V)	oxidation current (Amp)	Reduction current (Amp)
5 min.	-0.158	-0.175	-0.197	0.0147	-0.0256
10 min.	-0.219	-0.209	-0.162	0.0214	-0.0312
15 min.	-0.221	-0.223	-0.092	0.0234	-0.0401

Treatment of surface by cold plasma BDB

The best samples prepared from Cu/ITO were chosen in terms of compositional, surface and optical properties. The third sample, CCuITO, was the best for the purpose of cold plasma treatment. Table (2) shows the conditions for treating the selected sample with cold plasma, where the Argon element was used at a pressure of 8.5×10^{-1} mbar show figure (1)

Figure(1) :Schematic of a two-electrode electrode position cell

Table (2) Explains the conditions for treating the surface of the CCuITO sample with cold plasma

Thin film name CCuITO	Current mA	voltage volt	Exposure time in minutes
10CCuITO	10	500	10
20CCuITO	10	500	20
30CCuITO	10	500	30

Results:

X-ray diffraction examinations

Figure 2. It shows an X-ray diffraction diagram of a sample of copper films (CCuITO) deposited on bases of tin oxide doped with indimium ITO, which were treated with cold plasma for (10, 20, and 30) minutes in the presence of argon. The X-ray diffraction results of the sample treated at three times showed the appearance of three phases: the first is copper, tin oxide, and the third is indium oxide. The Cu peaks were at θ2 (43.15◦, 50.3◦), which correspond to the (111) and (002) levels according to reference (98-005-). 3758) and the phase is cubic, while the SnO peaks were at 2θ (36.25 and 35.1), which correspond to levels (200) and (102), and the phase was hexagonal according to reference (98-018-1283), while the InSnO peaks were at the corners (61.35, 30.18). which corresponds to levels (1-11) and (125) and the orthombic phase, according to the reference (98-016-1248)]. Table (3) shows the values of crystal size, density of dislocations, and crystal stress, in addition to the width of the peaks, noting that these values were calculated from equations (2-2, 2-3, and 2-4). In order to investigate the crystal lattice information and crystal size of copper films prepared under time-varying conditions with cold plasma. From these diffraction patterns shown in Figure (3) we notice from Figure 4-20 that the level of rotation differed from one sample to another, as shown in Table 4-5.

We note from Table (3) that crystallinity increased with increasing plasma treatment time for the first and second samples, then decreased back to 30.17 nanometers for the third sample, where the crystalline size increased from 32 to 48.77 nanometers. We also notice from Table (3) that the density of the dislocations increased from 9.29 x 1014 lin/m2 to 4.21 x 1014 lin/m2, except for the third sample, 30CCuITO, where the density of the dislocations increased. The reason can be attributed to the increased influence of ions as a result of the increased exposure time, which led to an increase in the density of the dislocations. As for the crystal stress, it decreased for the first and second samples from 0.004 to 0.0027, while it increased to 0.0044 for the third sample. The reason can be attributed to the plasma treatment and its effect on the surface of the sample. This behavior is consistent with the reference in the same line of research [11]. It is observed that with increasing processing time, the Ag diffraction peaks increase and become sharper. The increase in peak intensity may be due to the increase in crystalline size shown in Table (3).

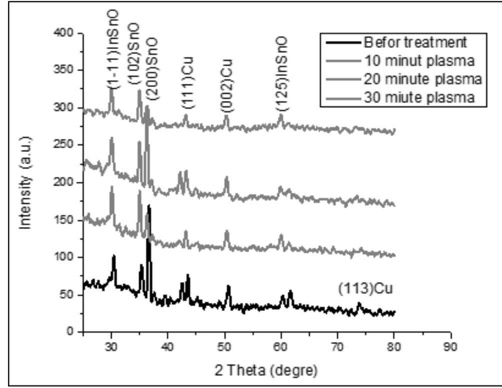

Figure (2) shows X-ray diffraction diagrams of copper films before and after cold plasma treatment.

Table (3) shows X-ray diffraction parameters of prepared copper films

Crystallographic Parameters	Sample before processing CCuITO	sample 10CCuITO	sample 20CCuITO	sample 30CCuITO
2θ	36.2	35.1	36.14	35.01
d_{hkl}	1.8803	2.5506	1.8853	2.5401
FWHM	0.3554	0.2023	0.2017	0.3214
Disloca ITOn δ (nm)	$9.29x10^{14}$	$4.43x10^{14}$	$4.21x10^{14}$	$1.1x10^{15}$
Lattice strain ε (%)	0.004	0.0028	0.0027	0.0044
Crystallite size D (nm)	32	47.99	48.77	30.17

Atomic force microscopy (AFM) examinations

Figure (3) shows three-dimensional AFM images of copper films treated with plasma at different times (10, 20, 30) minutes. Table (4) shows the values of particle size distribution, surface roughness, and RMS for copper membranes. We notice that the particle size distribution increased after treatment with plasma, reaching 0.119 micrometers for the sample treated for 10 minutes. Then it decreased from this value for the second sample, reaching 0.117 micrometers, then increasing again for the third sample, 30CCuITO, reaching 0.125 micrometers. The reason for this can be attributed to the collision between the argon ion and the surface. Copper after exposure to plasma, which causes a corrosion state that increases the roughness of the coating and increases the agglomeration of grains on the surface [12]. We also notice from Table 4-4 that the roughness of the average granular free radical increased after treatment with plasma, reaching 81.52 nm for the sample treated for 10 minutes. Then it decreased from this value for the second sample, reaching 69.444 nm, then increasing again for the third sample, 30CCuITO, reaching 108.899 nm. The reason can be attributed to the effect of Arcon ion on the membrane surface. These results are consistent with the researcher's findings [13].

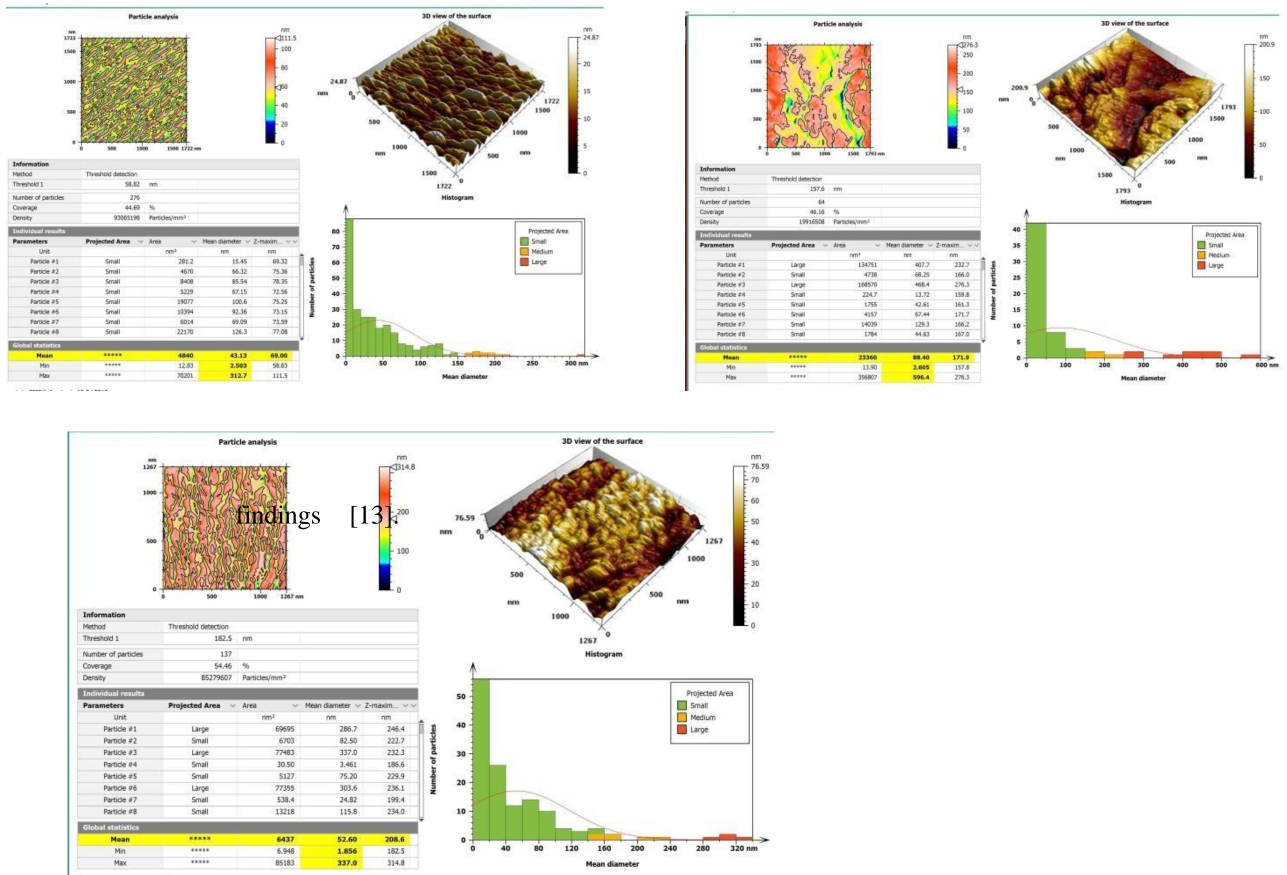

Fig (3) Atomic force microscope images of plasma-treated samples with a plot of the grains on the surface and the distribution profile.

Table (4) represents the parameters of the atomic force microscope images of the prepared samples

Sample name	Distribution of granular size on the surface	Roughness nm	RMS nm
CCuITO	0.0903 nm	66.074	81.236
10CCuITO	0.119 µm	67.003	81.52
20CCuITO	0.117 µm	53.550	69.444
30CCuITO	0.125 µm	87.771	108.899

SEM examinations

The SEM image of Cu particles after plasma treatment at different times is shown in Figure(4). The images show the presence of clumps that increase with increasing plasma treatment time, which indicates surface corrosion as a result of the collision of the argon ion with the surface of the membrane. The particle size for the untreated sample was 84.285 nm, while for the samples treated with plasma at times 10, 20, and 30, it was 82.2 nano, 87 nano, and 105 nm. Nano respectively, which indicates that the granular size increases with increasing treatment time. It can also be observed from

the images that agglomeration also increases, knowing that agglomerations were neglected from particle size measurements, and this is consistent with reference [15,14].

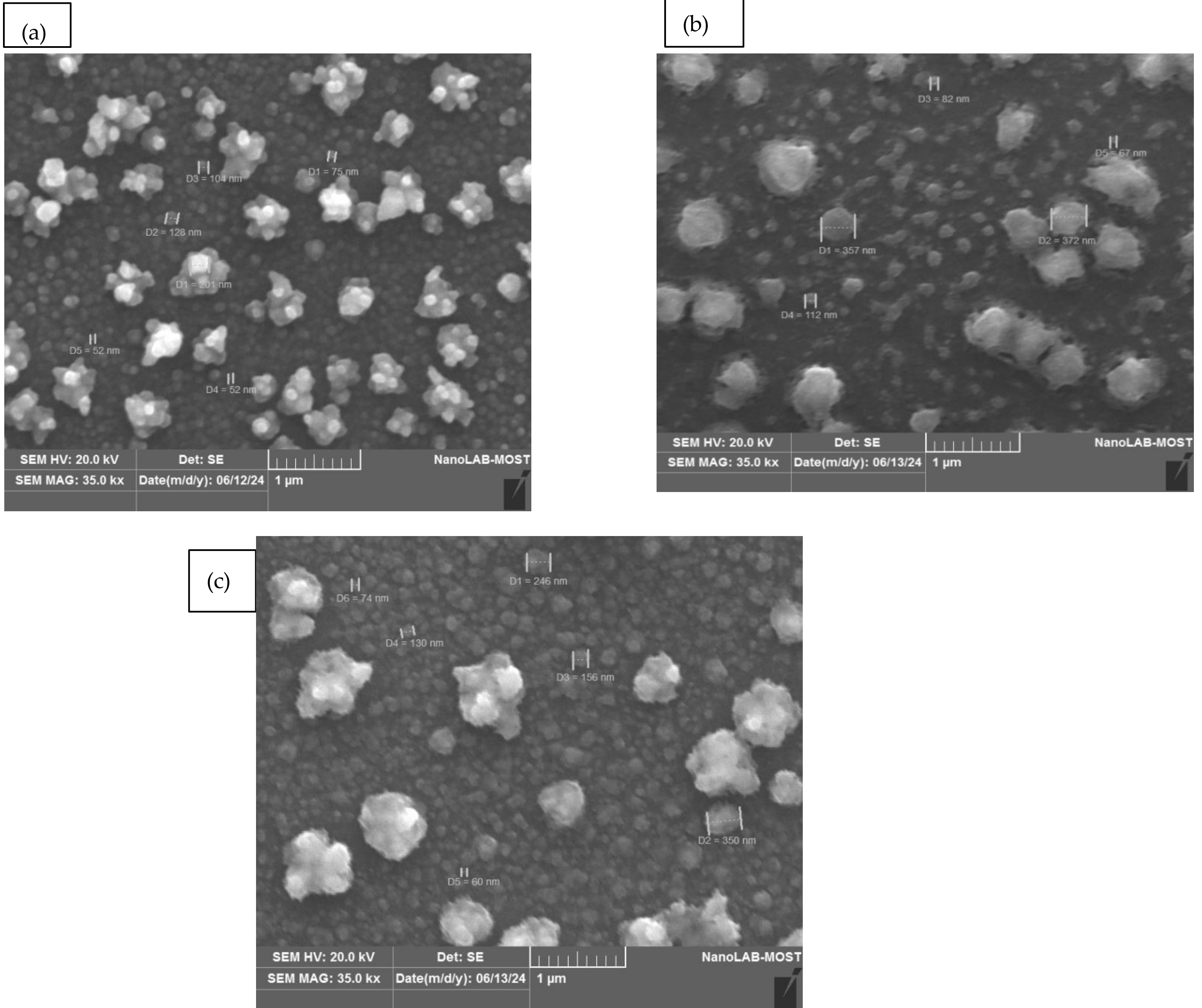

Figure (4) 10CCuITO, (b) 20CCuITO, (c) 30CCuITO

Conclusion•

X-ray diffraction tests showed the appearance of three different phases, SnO2, InSO2, and Cu. The crystallization size increased for the 20CCuITO sample to reach 48.77 nm, while it decreased for the 30CCuITO sample to reach 30.17 nm. It can be concluded that the plasma treatment improved the crystallization size by an amount of 0.5 compared to the untreated sample. With plasma, which was 32 nm. The results of the AFM images showed that the grain size distribution rate was the least for the 20CCuITO sample and the largest for the 30CCuITO sample. SEM image results showed that the grain size increased with increasing plasma treatment time, rising from 82.2 to 105 nm with an increase in agglomerations compared to the untreated sample

Author Contributions: mohammed Shareef mohammed : helps in collecting and analyzing data .participated in the literature review and provided feedback on drafts of the manuscript, Review and edit the final manuscript for clarity and consistency and Methodology.

Funding: Please add: The authors declare that no funding was received.

Data availability statement: The data underlying the results presented in the study are available within the manuscript.

.

Data Availability Statement: The data underlying the results presented in the study are available within the manuscript

Conflicts of Interest The authors declare that they have no conflicts of interest regarding the publication of this paper

References

References

1. Dimitrakellis, P., Faubert, F., Wartel, M., Gogolides, E., & Pellerin, S. (2022). Plasma surface modificaITOn of epoxy polymer in air DBD and gliding arc. *Processes*, *10*(1), 104.
2. Luisa Peraldo Bicelli, Benedetto Bozzini, Claudio Mele and Lucia D'Urzo, A Review of Nanostructural Aspects of Metal Electro-deposiITOn, Int. J. Electrochem. Sci., 3, 2008, 356 – 408
3. A.Milchev, ElectrocrystallizaITOn: Fundamentals of NucleaITOn and Growth, (Kluwer Academic Publishers,The Netherlands, 2002)
4. M Schlesinger and M Paunovic, Modern Electroplating (John Wiley and sons 5th ediITOn, 2011)9.
5. AHMED, Zouaoui. Electrodeposited copper on indium tin oxide. ReacITOn and nucleaITOn mechanisms. *Academic Perspective Procedia*, 2018, 1.1: 565-571.
6. A. Mallik and B. C. Ray, EvoluITOn of principle and practice of electrodeposited thin film: A Review on effect of temperature and sonicaITOn, InternaITOnal Journal of Electrochemistry 16, 2011.
7. E. García, Mario Romero-Romo, María Teresa Ramírez-Silva, and Manuel Palomar-Pardavé, Overpotential NucleaITOn and Growth of Copper onto Polycrystalline and Single Crystal Gold Electrodes, Int. J. Electrochem. Sci., 7, 2012, 3102 – 3114.
8. F A Lowenheim, Modern Electroplating, (J. Wiley and sons, New York , 1974).
9. Darko Grujicic and Batric Pesic, ElectrodeposiITOn of copper: the nucleaITOn mechanisms, Electrochimica Acta 47, 2002, 2901-291.
10. J.C. Ballesteros, E. Chainet, P. Ozil, Y. Meas and G. Trejo, ElectrodeposiITOn of copper from noncyanide alkaline soluITOn containing tartrate, Int. J. Electrochem. Sci., 6, 2011, 2632 – 2651.
11. Singho, N. Johan, M. & CheLah, N. 2014. " Temperature-dependent properties of silver-poly (methylmethacrylate) nanocomposites synthesized by in-situ technique", Nanoscale Research Letters, vol.9, pp.1-6.
12. Reece, R.J. 2001. Industrial plasma engineering, vol. 2. ApplicaITOns to Nonthermal Plasma Processing, Bristol and Philadelphia: Institute of Physics Publishing; pp. 337.

13. Abdel-Khalek, H., El-Samahi, M. I., & El-Mahalawy, A. M. (2018). Plasma impact on structural, morphological and optical properties of copper acetylacetonate thin films. *Spectrochimica Acta Part A: Molecular and Biomolecular Spectroscopy*, *199*, 356-366.

14. Lim, J. D., Lee, P. M., Rhee, D. M. W., Leong, K. C., & Chen, Z. (2015). Effect of surface treatment on adhesion strength between magnetron sputtered copper thin films and alumina substrate. *Applied Surface Science*, *355*, 509-515.

15. Park, M., Baek, S., Kim, S., & Kim, S. E. (2015). Argon plasma treatment on Cu surface for Cu bonding in 3D integraITOn and their characteristics. *Applied Surface Science*, *324*, 168-173.